Optics Communications 380 (2016) 35–40

Contents lists available at ScienceDirect

Optics Communications

journal homepage: www.elsevier.com/locate/optcom

Experimental demonstration of fractional order differentiation using a long-period grating-based in-fiber modal interferometer

L. Poveda-Wong [a], A. Carrascosa [a], C. Cuadrado-Laborde [b,c,*], J.L. Cruz [a], M.V. Andrés [a]

[a] Departamento de Física Aplicada y Electromagnetismo, ICMUV, Universidad de Valencia, C/Dr. Moliner, 50, Burjassot 46100, Spain
[b] Instituto de Física Rosario (CONICET-UNR), Bulevar 27 de Febrero 210bis, S2000EZP Rosario, Santa Fe, Argentina
[c] Pontificia Universidad Católica Argentina, Facultad de Química e Ingeniería, Av. Pellegrini 3314, S2000BPN Rosario, Santa Fe, Argentina

ARTICLE INFO

Article history:
Received 7 March 2016
Received in revised form
28 April 2016
Accepted 29 May 2016

Keywords:
Fractional differentiation
Fiber optics
Mach–Zehnder
Long-period grating

ABSTRACT

In this work we demonstrate both, experimentally and theoretically, that a long-period grating-based in-fiber modal interferometer can perform an all-optical arbitrary-order fractional differentiation. Experimentally, we fractionally differentiated to the 0.5th order a secant hyperbolic-like pulse of 23 ps time width provided by a 1039.5 nm emission wavelength modelocked fiber laser, with a chirp parameter of −30. An analytical expression relating the fractional order of differentiation n with the characteristics of the modal interferometer was also derived, with the purpose to simplify the design procedure. The proposal was corroborated also numerically. This device may find applications in real time phase recovery.

© 2016 Elsevier B.V. All rights reserved.

1. Introduction

A photonic temporal differentiator is a device that provides the time derivative of the complex envelope of an arbitrary input optical waveform. The device may find interesting applications for optical pulse shaping, optical computing, information processing systems, and ultra-high-speed coding, among other uses. In the last few years different proposals were presented to perform all-optical differentiation [1,2]. Generally, the in-fiber way is preferred, because it offers simplicity, low cost, low insertion loss, and inherent full compatibility with fiber optic systems. These proposals only took into account integer order differentiation up to 2008, were the first in-fiber fractional order differentiation was proposed [3]. Since then, several proposals were made to perform fractional differentiation based on in-fiber technology [4–6]. Between them, the fiber Bragg grating (FBG) approach is generally well-suited to process input bandwidths below 20 GHz; higher processing bandwidths would imply impractically shorter FBGs [4]. On the other hand, the long period grating (LPG) approach is best adapted to process THz-bandwidth input signals [5]. Therefore, there is a bandwidth gap to be covered for these kinds of devices. Although it could be possible to process lower-bandwidth signals using the LPG approach, this would result in a very low energetic efficiency – i.e. the power ratio between the differentiated and original signals –, which would severely increase the signal-to-noise ratio. Further, the spectral matching between the input light pulse to be processed and the photonic fractional differentiator becomes more critical in the fractional order case than in its integer order counterpart. This is, because in the fractional order case, there is not the required phase discontinuity at the operation wavelength, but a smooth phase transition in a narrow spectral bandwidth [4]. Therefore, in the experimental realizations of fractional order differentiators, there is a minimum spectral bandwidth for the input signal to be processed. For this reason, it becomes important to provide fractional differentiator order solutions covering this bandwidth gap, between GHz and THz, in order to process different light waveforms.

In this work we propose an in-fiber fractional differentiation well suited to process input optical signals in this gap bandwidth between 20 GHz and 200 GHz and beyond. It has been recognized before, the ability of interferometric techniques to perform integer-order differentiation [7]. In Ref. [3] it was demonstrated that an asymmetrical and unbalanced Mach–Zehnder interferometer (MZI) has a spectral transfer function similar to that required to perform fractional order differentiation. The setup proposed here is a modal MZI defined by a pair of LPGs written sequentially in the same piece of an (stripped) optical fiber, which exhibits a highly stable response. One key advantage of the proposed implementation is its increased stability versus environmental fluctuations, particularly as compared with a direct implementation of

* Corresponding author at: Instituto de Física Rosario (CONICET-UNR), Bulevar 27 de Febrero 210bis, S2000EZP Rosario, Santa Fe, Argentina.
E-mail address: christian.cuadrado@uv.es (C. Cuadrado-Laborde).

http://dx.doi.org/10.1016/j.optcom.2016.05.083
0030-4018/© 2016 Elsevier B.V. All rights reserved.

a MZI structure in an all-fiber configuration [3]. In the proposed LPG-based device, both arms of the interferometer are simultaneously exposed to nearly identical environmental variations, thus greatly increasing the device stability. These LPGs establish a coaxial MZI for fiber modes propagating through the core and cladding in the same direction. In a sense, this work could be considered a generalization of Ref. [8], in which a LPG MZI was presented, but only for integer order differentiation purposes. Further, with the purpose to alleviate the design process, different analytical expressions are derived, relating the required spectral characteristics for nth order fractional differentiation with the LPG MZI parameters. As a proof of concept, we successfully demonstrates experimentally, the 0.5th order fractional differentiation of a secant hyperbolic-like pulse of 23 ps time width provided by a 1039.5 nm emission wavelength modelocked fiber laser, with a chirp parameter of -30. Finally, different numerical simulations describe the design and performance of a 0.82th order device at 1555 nm.

2. Theory

It is well known that the Fourier transform of a signal $F(\nu) = \Im\left[f(t)\right]$ and its nth time derivative $F_n(\nu) = \Im\left[d^n f(t)/dt^n\right]$ are related by [3,4]:

$$F_n(\nu) = (j2\pi\nu)^n F(\nu), \tag{1}$$

where $n \in \Re^+$, and ν is the baseband frequency, i.e. $\nu = (\omega - \omega_0)/2\pi$, with ω the optical angular frequency variable, and ω_0 is the optical carrier angular frequency. From Eq. (1), we could consider as well the process of differentiation as a filtering action performed by an ideal filter $H_n(\nu) = (j2\pi\nu)^n$ on the input signal spectrum $F(\nu)$. Thus, a nth order fractional differentiator requires a $\Delta\theta = n\pi$ phase discontinuity at $\nu = 0$, and a $|\nu|^n$ dependence for the amplitude of the transfer function.

In Ref. [3] it was demonstrated that an asymmetrical and unbalanced MZI – i.e. splitting/coupling ratio different of 1/2 and different length paths – has a spectral transfer function that resembles the required for fractional order differentiation. A MZI is a four ports device; there are two input ports and two output ports. Usually, it is created from two couplers connected by arms of unequal optical lengths. The output ports are usually called as bar and cross ports, depending if most of the light appears in the same waveguide of the input or not, respectively. In a LPG MZI, the inputs and outputs are two fiber modes at the beginning and end of the optical fiber section in which the device is constructed; thus, the arms of the interferometer are typically the LP_{01} core mode and the LP_{0m} cladding mode excited by the LPG, see Fig. 1. In the following, we will assume that only the core guided mode is initially excited by the pulse launched at the input of the LPG MZI. The first LPG couples a certain amount of power from the core to the cladding, characterized by ρ_1, with $0 \le \rho_1 \le 1$. After light propagates by both arms, the second LPG couples back to the core a certain amount of power from the cladding, characterized by ρ_2, with $0 \le \rho_2 \le 1$; where it is finally coherently recombined with the light propagated by the core, not coupled to the cladding by the first LPG. In a LPG MZI both arms have the same length; it is the difference between the core and cladding mode-propagation constants β_i which induces a time delay τ. In the following, we will focus exclusively in the output bar port, since we are not interested in the possibility to recover light from the cladding (cross port). By the transfer matrix formalism, it is easy to show that the transfer function for the bar port is given by [9]:

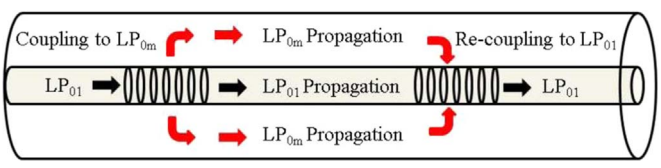

Fig. 1. Scheme of the proposed fractional differentiator based on the use of a LPG MZI.

$$B(\nu) \equiv 1 - \chi\exp(j2\pi\nu\tau), \tag{2}$$

where the pre-exponential factor χ is related with the power splitting ratios through:

$$\chi^2 = \frac{(1-\rho_1)(1-\rho_2)}{\rho_1\rho_2}. \tag{3}$$

The amplitude response of the bar port transfer function $B(\nu)$ presents periodically transmission dips at frequencies given by $\nu = m/\tau$ – with $m \in \mathbb{Z}$ – together with a maximum phase change $\Delta\theta$. Due to this periodic behavior, we can consider the difference between interference fringes as the maximum operative bandwidth of the MZI $\Delta\nu_{BW} = 1/\tau$. The relationship linking $\Delta\theta$ with χ, can be obtained by finding the maximum/minimum in the phase of $B(\nu)$, see Eq. (2). Following this procedure, we arrive to the following equality [3]:

$$\chi = \frac{\tan(\Delta\theta/2)}{\sqrt{\tan^2(\Delta\theta/2)+1}}. \tag{4}$$

Eq. (4) admits multiple solutions, since χ is a function of two variables, see Eq. (3). However, by arbitrary fixing the power splitting ratio of the first LPG $\rho_1 = 1/2$, and by using Eqs. (3) and (4), the power splitting ratio of the second LPG can be expressed as a function of the fractional differentiator order through:

$$\rho_2 = \frac{1}{2} + \frac{1}{2}\left[2\tan^2\left(\frac{\pi n}{2}\right)+1\right]^{-1}, \tag{5}$$

where $\Delta\theta$ is written as a fraction n of π; i.e., $\Delta\theta = n\pi$. Fig. 2 shows the relationship between ρ_2 and n; as expected when $\rho_2 = 1/2$, we have a first-order differentiator [7,8]. According to Eqs. (4) and (5), it is possible to obtain any arbitrary phase change $\Delta\theta$, just adequately choosing the second power-splitting ratio ρ_2, when ρ_1 is arbitrary fixed. However, it is worth nothing that the MZI does not present exactly the required $n\pi$ phase discontinuity, but a maximum phase change $\Delta\theta = n\pi$ in a bandwidth $\Delta\nu_\theta$ given by the spectral positions of the maximum/minimum of the phase of $B(\nu)$:

$$\Delta\nu_\theta = \Delta\nu_{BW}\left(\frac{1-n}{2}\right), \tag{6}$$

which has been obtained by using Eqs. (4) and (5). As expected, when $n = 1$, $\Delta\nu_\theta = 0$; i.e. there is a phase discontinuity, as it has been demonstrated before for integer order differentiation [1,2,7,8]. Following Eq. (6); as the fractional differentiator order n increases, the ratio between the bandwidths of the phase transition and the maximum operative bandwidth $\Delta\nu_\theta/\Delta\nu_{BW}$, linearly decreases; see Fig. 2(b). In other words, the useful spectral bandwidth – which is restrained between $\Delta\nu_\theta$ and $\Delta\nu_{BW}$ – increases as the fractional differentiator order approaches one. In the other limit for $n \to 0$, the bandwidth of the phase transition approaches half the full operative bandwidth. In conclusion, for an optimal performance, the bandwidth of the input optical signal should be higher than the phase transition bandwidth $\Delta\nu_\theta$, but lower than the maximum operative bandwidth $\Delta\nu_{BW}$.

3. Results

In the following, we first show the experimental 0.5th order fractional differentiation of a light pulse provided by a 1039.5 nm

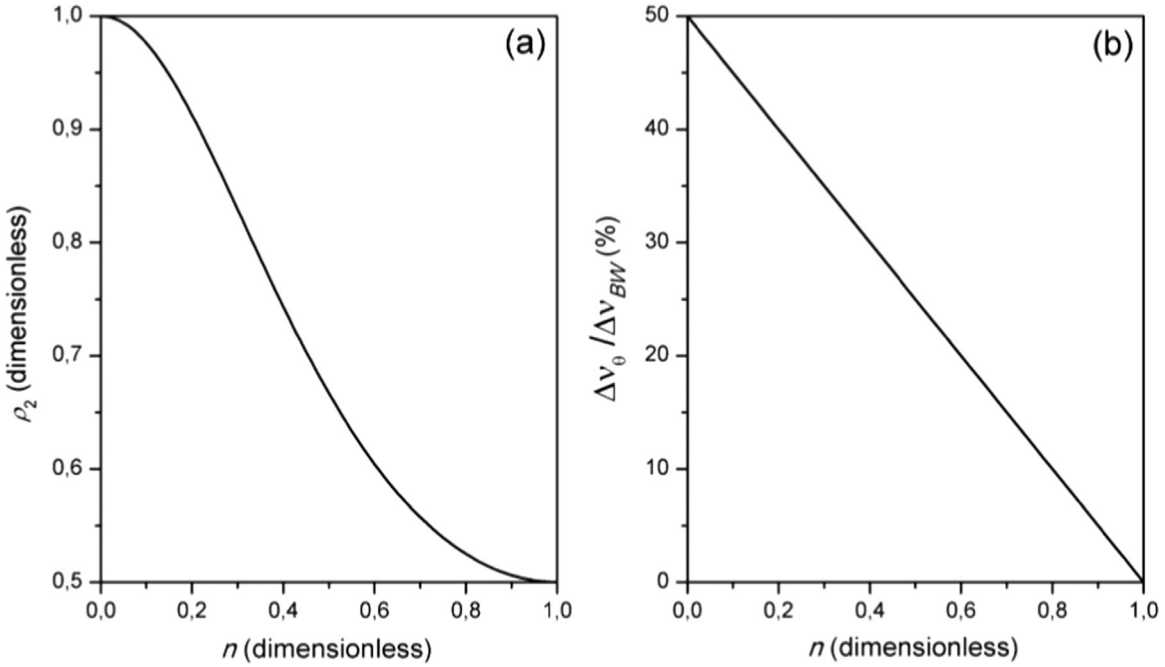

Fig. 2. (a) Power splitting ratio of the second LPG ρ_2 as a function of the fractional order n of the differentiation, for $\rho_1=0.5$. (b) Ratio between the bandwidth of the phase transition $\Delta\nu_\theta$ and the maximum operative bandwidth $\Delta\nu_{BW}$, as a function of the fractional differentiation order n.

emission wavelength modelocked fiber laser by using a LPG MZI, Section 3.1. Next, the design and performance of a 0.82th order fractional differentiator using a LPG MZI, which works at 1555 nm, is shown, through several numerical examples, Section 3.2.

3.1. Experimental results

The LPG MZI was constructed by recording two different LPGs in a single piece of a boron-doped photosensitive fiber (PS980 by Fibercore, numerical aperture of 0.13 and cut-off wavelength of 980 nm), by using the point-by-point technique. The selected periodicity for both LPGs was of 189.7 μm. In one of the LPGs (LPG_1) the number of periods was 28, resulting in a total length of 5.3 mm for LPG_1. The transmission response for LPG_1 was followed during the fabrication process by measuring the transmitted light provided by a led source in an optical spectrum analyzer (spectral resolution 20 pm). The recording of LPG_1 was interrupted when the transmission reached a resonance depth of −3 dB (i.e., $\rho_1=0.5$) at 1039.8 nm. Next, LPG_2 was recorded slightly shorter; i.e., 25 periods, giving a LPG_2 length of 4.7 mm (with the remaining recording parameters unchanged, as compared with LPG_1). As a consequence of this, the estimated transmittance dip for LPG_2 was of −1.8 dB, i.e. $\rho_2=0.66$. Following Fig. 2, this combination between ρ_1 and ρ_2 corresponds to a fractional order differentiator of 0.5th order. On the other hand, the separation between LPGs is determined by the required operation bandwidth, which in turn is fixed by the spectral characteristics of the input optical signal to be processed, which should be known *a priori*. In our case, the optimum processing bandwidth was achieved, by selecting a distance between LPGs of 65 mm (center-to-center distance). Fig. 3 shows the observed interference pattern in the optical spectrum analyzer (in transmission), when the LPG MZI is illuminated by a led source. The central peak of transmission minimum is located at 1039.8 nm; whereas the operation bandwidth – which is given approximately by the separation between the transmission maxima at each side of the central peak of transmission minimum – is around 3 nm, see Fig. 3. This value determines the maximum operative bandwidth $\Delta\nu_{BW}=83$ GHz.

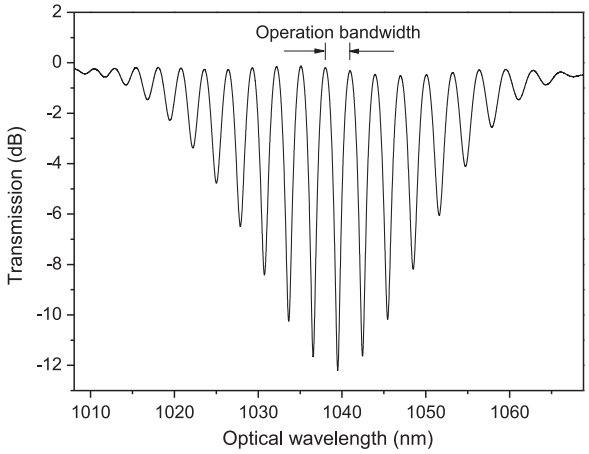

Fig. 3. Measured spectral power transmission of the LPG MZI. The device works as a 0.5th order fractional differentiator in the central spectral region.

The light pulses to be optically differentiated were provided by a passively modelocked ytterbium fiber laser, emitting at a fixed wavelength $\lambda_0=1039.5$ nm. However, it was necessary to shift the operation wavelength of the LPG MZI to the emission wavelength of the laser, by mounting the LPG MZI on a micrometric translational stage (distance between clamps 145 mm). The repetition rate of the modelocked laser was of 23.15 MHz, and the output light pulses can be approximately fitted with an hyperbolic secant profile $f(t)=\mathrm{sech}(t/T_0)$, with $T_0=13$ ps, i.e., a FWHM of 23 ps, see Fig. 4(a). Since the output light pulses provided by our modelocked laser are severely chirped, we found essential to monitor its instantaneous angular frequency profile also. To this end, we used the phase recovery technique proposed in Ref. [10] (not shown). As a result, we found a parabolic phase profile for the output pulse of the modelocked laser $f(t)$, which can be approximately described by $\exp(-jCt^2/2T_0^2)$, where C is the chirp parameter, being $C=-30$ according to our fitting. Fig. 4(b) shows the spectra of the light pulses at the input and output of the LPG MZI. One can see that the input signal carrier is well aligned with the central resonance

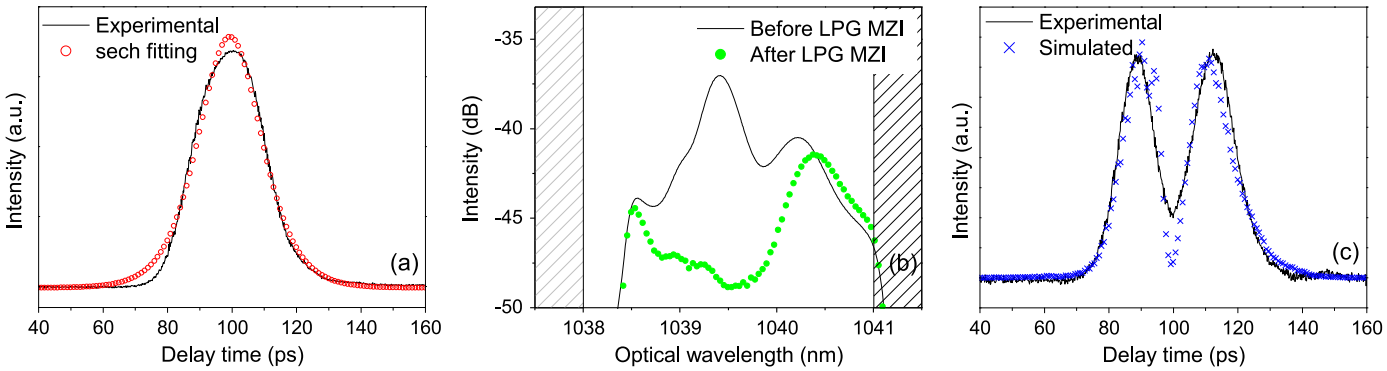

Fig. 4. (a) Temporal intensity profile at the input of the LPG MZI, together with its corresponding fitting. (b) Spectra of the light pulse before and after the LPG MZI. (c) Temporal intensity profile at the output of the LPG MZI, together with the simulated response of a 0.5th order fractional differentiator.

optical wavelength of the LPG MZI; as a result, the optical carrier is deeply suppressed in the output light pulse for more than 12 dB; see Fig. 4(b). Fig. 4(c) shows the measured temporal intensity profile at the output of the LPG MZI. In the same figure, it is also shown the simulated response of an ideal 0.5th order fractional differentiator, for comparison purposes. The input pulse of this simulation was composed with the square root of the measured temporal intensity profile as the modulus, and the reconstructed phase obtained above for $f(t)$. There is a good degree of resemblance between both experimental and simulated temporal profiles; the higher deviation is located in the minimum between intensity maxima of the twin peak (around 100 ps of delay time). This difference could be motivated by the limited bandwidth of the available detector. Finally, it is worth to remark, that the 0.5th order of the present device is rather precisely demonstrated by Fig. 4(c), since a differentiation of a different fractional order ($n \neq 0.5$), could be easily perceived in the oscilloscope trace through the temporal separation between the intensity peaks, increasing, as the fractional order increase, and *vice versa* [5].

3.2. Numerical results

In the following, a simulation further illustrates the design and performance of fractional differentiators using LPG MZI and operating at 1555 nm. The simulations for the LPG MZI were performed according to the coupled-mode theory, as in Ref. [11]. For the results presented here, we simulated a uniform MZI LPG written in the core of a SMF-28 optical fiber performing a 0.82th order fractional differentiation. The LPGs were designed to couple light between the fundamental core mode and the third cladding mode. The following parabolic wavelength dependence was assumed for the effective refractive indices corresponding to the core mode $n_0 = 1.46410 - 0.00830\lambda - 0.00185\lambda^2$ and the cladding mode $n_3 = 1.45769 - 0.00507\lambda - 0.002479\lambda^2$ [11]. The grating period was fixed to $\Lambda = 534.65$ μm, which translates into a central resonance wavelength of $\lambda_0 = 1555$ nm ($\nu_0 = 192.79$ THz). The LPG lengths was set in both cases to $l = 20$ mm, whereas the separation between LPGs was set to $L = 11 \times l$ (center to center distance). In this work we arbitrary fixed $\rho_1 = 0.5$, i.e. a transmissivity for the first LPG of -3 dB; which implies $\kappa_1 L_1 = \pi/4$, resulting in a coupling coefficient of $\kappa_1 = 39.27\ \mathrm{m}^{-1}$. According to Eq. (5), in order to perform a 0.82th order fractional differentiation, we need for the second LPG a $\rho_2 = 0.52$ – i.e. a transmissivity of -2.84 dB –, which is reached by using a slightly lower coupling coefficient of $\kappa_2 = 38\ \mathrm{m}^{-1}$. Both coupling coefficients are in accordance with standard experimental values currently achievable.

Fig. 5 shows the intensity transmission and phase response of the LPG MZI. As we explained above, the separation between the interference fringes of a LPG MZI, limits the maximum operative

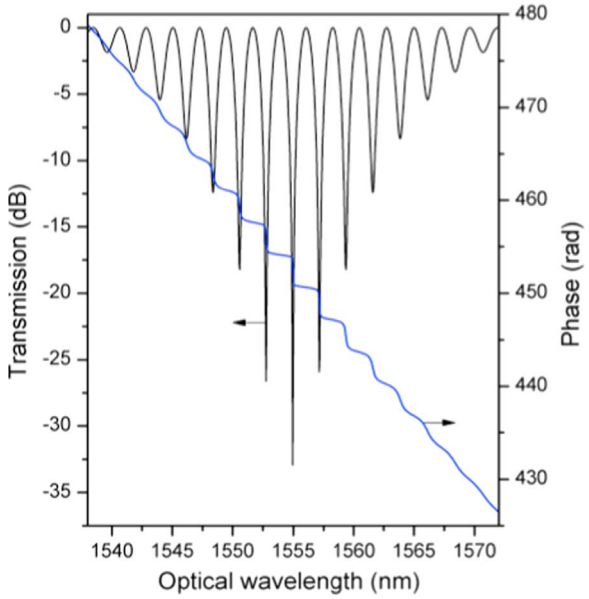

Fig. 5. Spectral power transmission and phase response of the 0.82th order fractional differentiator simulated in a SMF-28 optical fiber; LPGs are 20 mm each separated by 220 mm (center-to-center distance). Operative bandwidth: < 270 GHz.

bandwidth. This separation is inversely proportional to the delay time τ, which in turn depends on both the difference between core and cladding group velocities and the separation between LPGs [12]. On the other hand, the group velocity is determined by the phase velocity (characterized by the effective refractive index of the mode) and the modal dispersion. In this specific example the separation between transmission minima is of 270 GHz, which can be taken roughly as the maximum operative bandwidth. Fig. 6 shows a detail of the central interference fringe in intensity and phase response. It can be observed a maximum phase change $\Delta\theta = 2.57$ rad, which can be associated with a fractional differentiator order $n = \Delta\theta/\pi = 0.82$, as expected. By using Eq. (6) with $\Delta\nu_{BW} = 270$ GHz, this phase change takes place in a spectral bandwidth of $\Delta\nu_\theta = 24$ GHz. For comparison purposes, Fig. 6 also shows the ideal transfer function for a fractional differentiator order $n = 0.82$, i.e. $(j2\pi\nu)^{0.82}$. The degree of resemblance between the proposed and the ideal transfer functions is acceptable, provided the frequency band of the signal matches adequately the central part of the transfer function. The bandwidth of the input optical signal should be higher than the bandwidth of the phase change; i.e., 24 GHz; but lower than the maximum operative bandwidth; i.e., 270 GHz.

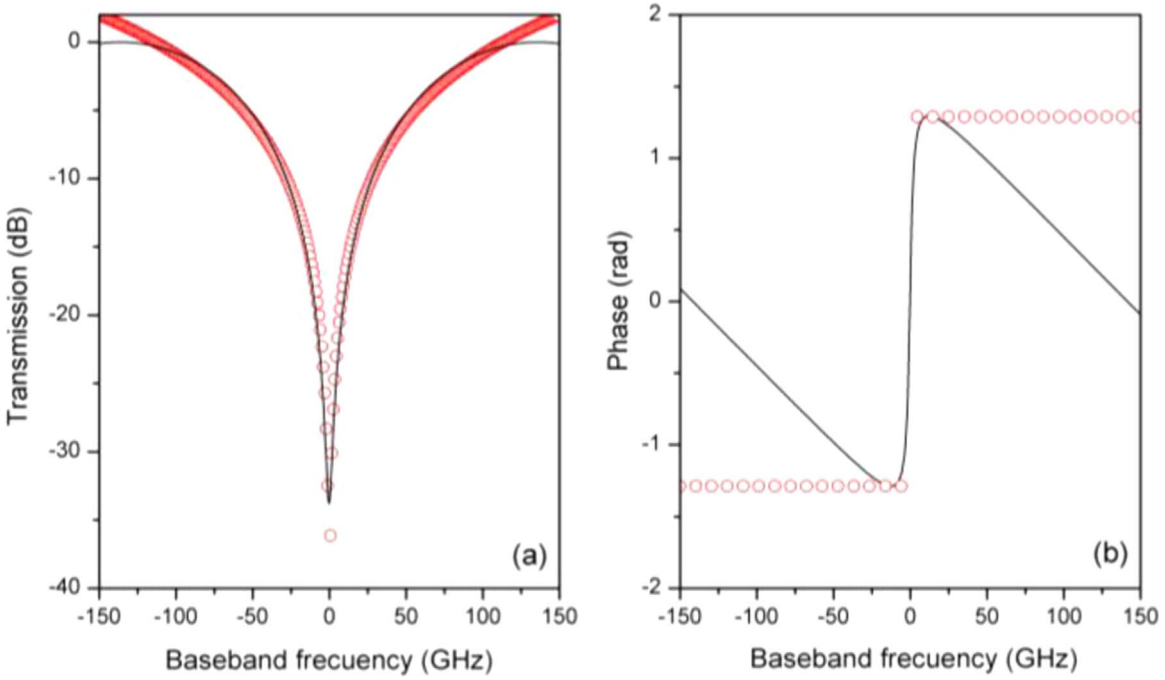

Fig. 6. Detail of the central interference fringe shown in Fig. 5. Simulated (solid line) and ideal (open scatter points) spectral behavior of the 0.82th order fractional differentiator in transmission and phase, (a) and (b), respectively. The average group delay of the LPG MZI was subtracted in (b).

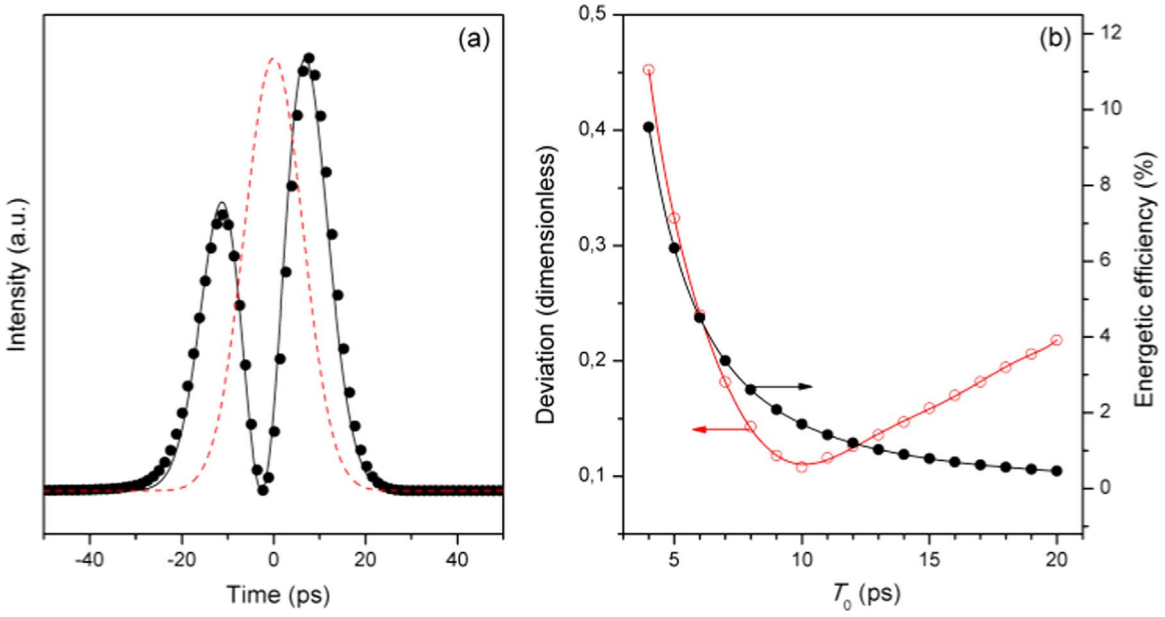

Fig. 7. (a) Simulated (solid curve) and ideal (solid scatter points) time response of the designed 0.82th-order fractional differentiator for an input Gaussian pulse (dashed curve). All signals were normalized to unity in order to facilitate the comparison between them. (b) Deviation factor and energetic efficiency of the proposed 0.82th order fractional differentiator as a function of the time width of the input signal.

To prove the proper performance of this device, we have numerically simulated its time-domain response. Numerical calculations were performed in a time window of 534 ps with 1.7×10^4 points equally spaced (time discretization). We use a Gaussian pulse as input signal $f(t)=\exp[(-1/2)(t/T_0)^2]$, with $T_0=7$ ps, i.e. a FWHM of 11.6 ps and a spectral bandwidth of 38 GHz (FWHM). Fig. 7(a) shows the input signal, the output of the LPG MZI 0.82th-order differentiator, and the ideal fractional time derivative. There is a good agreement between the obtained time profile at the output of the LPG MZI, and the theoretical time derivative. However, in order to make feasible a quantitative analysis, we defined a dimensionless deviation factor, as in Eq. (7) of Ref. [3]. This was estimated as the absolute value of the relative difference between the normalized optical intensities of the proposed and the ideal temporal derivatives, evaluated over the full computational time window. The deviation factor for this specific example was of 0.12. When evaluating this performance, two points should be considered. First, in an ideal fractional differentiator the transmittance dip would decay $-\infty$ dB, whereas in the proposed fractional differentiator it decays -34 dB, therefore low frequency components are not adequately rejected. Second, in an ideal fractional differentiator there is a phase discontinuity around the resonance frequency, whereas here the phase changes continuously in a spectral bandwidth of 24 GHz. Despite both drawbacks, the performance

can still be considered acceptable, as Fig. 7(a) shows. We also estimated the energetic efficiency as the ratio between the total optical power at the differentiator output and input, it was of 2.1%. This low value is typical for optical differentiation.

Next we analyzed the sensitivity of this setup under a change of the bandwidth of the input signal, see Fig. 7(b). To this end, we used several input Gaussian signals with temporal widths ranging from 4 ps $\leq T_0 \leq$ 20 ps – i.e. an spectral bandwidth ranging from 67 GHz to 13 GHz (FWHM) –, and the same LPG MZI design used before, i.e. $n=0.82$. The optimum optical input bandwidth can be selected from this figure for a given required precision, i.e. deviation factor. Fig. 7(b) also shows the energetic efficiency for each specific time width of the input signal.

On the other hand, based on the spectral behavior shown in Figs. 3 and 5, the reader could be inclined to assume that this device is a natural candidate to process wavelength division multiplexed (WDM) signals. However, it is worth to say, that this is not the case; because, although in amplitude the periodical behavior is approximately attained, it is not in phase. The successive resonance frequencies at each side of the central peak present a monotonously decreasing maximum phase change; i.e., each dip performs a fractional differentiation of different orders. This behavior makes unfeasible a simultaneous differentiation of a multiple WDM signal with a single fractional order. However, this could be useful to implement different fractional differentiation orders using the same device by simply tuning the central wavelength of the signal to be processed. This may enable the realization of a photonic differentiation with discrete reconfigurable orders.

4. Conclusion

We analyzed the possibility to perform an arbitrary order fractional differentiation with a LPG MZI. This analysis encompasses a theoretical, experimental and numerical work. From our analysis, we derived an analytical expression relating the order of the fractional differentiation with the LPG parameters. As a proof-of-concept, we experimentally differentiated a light pulse to the 0.5th order with a LPG MZI operating at 1039.5 nm. Finally, different numerical simulations describe the design and performance of a 0.83th order fractional differentiator at 1555 nm under a variety of situations.

Acknowledgments

The authors acknowledge financial support from the *Ministerio de Economia y Competitividad* of Spain and the *Fondo Europeo de Desarrollo Regional* (FEDER) – project TEC2013-46643-C2-1-R – and the *Generalitat Valenciana* – project PROMETEOII/2014/072. L. Poveda-Wong acknowledges financial support from the *Generalitat Valenciana* of Spain (Ref.: GRISOLIA/2013/001). The work of C. Cuadrado-Laborde has been partially supported by project PIP 112-2015-0100607-CO, CONICET, Argentina.

References

[1] N. Berger, B. Levit, B. Fischer, M. Kulishov, D. Plant, J. Azaña, Temporal differentiation of optical signals using a phase-shifted fiber Bragg grating, Opt. Express 15 (2007) 371–381.
[2] R. Slavík, Y. Park, M. Kulishov, R. Morandotti, J. Azaña, Ultrafast all-optical differentiators, Opt. Express 14 (2006) 10699–10707.
[3] C. Cuadrado-Laborde, All-optical ultrafast fractional differentiator, Opt. Quantam Electron. 40 (2008) 983–990.
[4] C. Cuadrado-Laborde, M.V. Andrés, In-fiber all-optical fractional differentiator, Opt. Lett. 34 (2009) 833–835.
[5] L. Poveda-Wong, A. Carrascosa, C. Cuadrado-Laborde, J.L. Cruz, A. Díez, M. V. Andrés, Long-period grating assisted fractional differentiation of highly chirped light pulses, Opt. Commun. 363 (2016) 37–41.
[6] H. Shahoei, J. Albert, J. Yao, Tunable fractional order temporal differentiator by optically pumping a tilted fiber Bragg grating, IEEE Photon. Technol. Lett. 24 (2012) 730–732.
[7] Y. Park, J. Azaña, R. Slavík, Ultrafast all-optical first- and higher-order differentiators based on interferometers, Opt. Lett. 32 (2007) 710–712.
[8] R. Slavík, Y. Park, D. Krčmařík, J. Azaña, Stable all-fiber photonic temporal differentiator using a long-period fiber grating interferometer, Opt. Commun. 282 (2009) 2339–2342.
[9] G.P. Agrawal, Applications of Nonlinear Fiber Optics, Academic Press, New York, 2001.
[10] C. Cuadrado-Laborde, A. Carrascosa, P. Pérez-Millán, A. Díez, J.L. Cruz, M. V. Andrés, Phase recovery by using optical fiber dispersion, Opt. Lett. 39 (2014) 598–601.
[11] M. Kulishov, J. Azaña, Long-period fiber gratings as ultrafast optical differentiators, Opt. Lett. 30 (2005) 2700–2702.
[12] B. Lee, J. Nishii, Dependence of fringe spacing on the grating separation in a long-period fiber grating pair, Appl. Opt. 38 (1999) 3450–3459.